

A DUAL STAGE LASER ABLATION SOURCE
FOR COLD ATOMS?

by

Michael Amonson

A senior thesis submitted to the faculty of
Brigham Young University
in partial fulfillment of the requirements for the degree of

Bachelor of Science

Department of Physics and Astronomy

Brigham Young University

April 2008

Copyright © 2008 Michael Amonson

All Rights Reserved

BRIGHAM YOUNG UNIVERSITY

DEPARTMENT APPROVAL

of a senior thesis submitted by

Michael Amonson

This thesis has been reviewed by the research advisor, research coordinator,
and department chair and has been found to be satisfactory.

Date

Scott Bergeson, Advisor

Date

Eric Hintz, Research Coordinator

Date

Ross L. Spencer, Chair

ABSTRACT

A DUAL STAGE LASER ABLATION SOURCE FOR COLD ATOMS?

Michael Amonson

Department of Physics and Astronomy

Bachelor of Science

We report on an experiment to measure the velocity distribution in an atomic beam generated using a two-stage laser ablation source. We use a Nd:YAG laser to ablate a calcium target. A probe laser beam at 423 nm crosses the atomic beam at 53° . Its frequency is swept across the calcium resonance transition. We use a PMT to detect laser-induced fluorescence collected using a lens and an interference filter. Initial results indicate that the atomic beam velocity is independent of the back ablation laser intensity. We also find that the beam velocity is consistent with a thermal temperature near the melting temperature of calcium. These findings are at variance with a recent publication.

ACKNOWLEDGMENTS

Thanks to Dr. Scott Bergeson for advice and support and to NSF for funding this research.

Thanks also to Trent Mouton, Scott Daniel, Wes Lifferth, and William Farmer for technical support.

Contents

Table of Contents	vi
List of Figures	viii
1 Background and Setup	1
1.1 Background	1
2 Experimental Design and Setup	3
2.1 Setup	3
2.1.1 Lasers	4
2.1.2 Internal Design	5
2.1.3 External Design	6
2.2 Vacuum Lid	6
2.3 Control box and Labview program	8
3 Data	10
3.1 First Setup	10
3.2 Second Setup	11
3.3 Thermodynamics	12
3.4 Data	14
4 Conclusion	16
4.1 Conclusions	16
Bibliography	17
A Labview program for running the target stepper motor	18
B Schematics for the stepper motors	23
C Motor mounts	26
D Maple work and formulae	32
E Hamamatsu 1P28 Photomultiplier Tube	38

F Additional information about the vacuum chamber's window ports 41

Index 42

List of Figures

2.1	Four mirrors that take vertically polarized light and create horizontally polarized light. The blue lines indicate the path of the probe laser.	4
2.2	First setup for the vacuum chamber	5
2.3	Dimensions for the Al lid	7
2.4	The control box is sitting below the HP Signal Generator	8
2.5	Rear view of the control box	9
3.1	Second setup for the vacuum chamber	11
3.2	Graph of fluorescence vs. time for atoms in the first setup. The point of measure for this graph is 3.5 cm from the sapphire disk. The back-ablating intensity is $I = 0.99 \text{ J/cm}^2$ (top panel), $I = 0.248 \text{ J/cm}^2$ (middle panel), and $I = 0.198 \text{ J/cm}^2$ (bottom panel). For the weakest intensity, only noise is visible.	14
3.3	Graph of fluorescence vs. time for atoms in the second setup. The point of measure for this graph is 4.0 cm from the sapphire disk. The prompt peak from atoms in the collimated beam is clearly seen on top of a broad background from isotropically scattered atoms.	15
A.1	Front panel for the control program	19
A.2	Diagram of program	20
A.3	Diagram of program	21
A.4	Diagram of program	22
B.1	Motor that turns the sapphire disk	24
B.2	Motor that turns the target	25
C.1	Mount for the target motor	26
C.2	Dimensions for target motor mount	27
C.3	The Holder is tightened onto the motor target motor's shaft. The	28
C.4	Rod that the Ca target is placed on. It sits inside the holder. The threads on the rod advance the target with each step of the motor.	29
C.5	Mount for the disk motor	30
C.6	Dimensions for disk motor mount	31

D.1	33
D.2	34
D.3	35
D.4	36
D.5	37
E.1	39
E.2	40

Chapter 1

Background and Setup

1.1 Background

Laser ablation is the ejection of atoms from an object by irradiating its surface with a pulsed laser. This method is commonly used for microscopic lithography, spectroscopy, and studies in fundamental physics. It is often used to make atomic and ionic beams of refractory metals. In two-stage laser ablation a laser ablates material onto a transparent substrate to form a thin film. The film is then back ablated to create an atomic beam. This technique can create an atomic beam with better collimation than ablation directly from a sample.

Our interest in two-stage laser ablation was motivated by a recent article by K. Alti and A. Khare [1]. Their paper described a highly collimated sub-thermal atomic beam generated using a dual-stage ablation source. Such a source would be ideal to use in our laser-cooling research. It would be more efficient than the thermal oven source we are currently using, which operates at 1000K and is weakly collimated. Moreover, a low-temperature collimated source would be ideal for ultra-trace atom detection, precision spectroscopy, laser-cooling, and a number of other experiments. It

would make precision spectroscopic measurements of refractory metals much simpler.

Alti and Khare measured the atomic velocity using indirect methods. They measure sub-sonic atomic beam velocities corresponding to temperatures well below ambient conditions. If this is right, it represents a major breakthrough for atomic spectroscopy. They argue that such low temperature atomic beams are possible because of a low fluence back-ablating laser.

We designed an experiment to test Alti and Khare's conclusions. Our experiment uses time-resolved laser-induced fluorescence measurements to characterize the atomic beam. By scanning the laser frequency across the atomic absorption line, we can determine both the average longitudinal velocity and the rms thermal velocity in the moving frame of the atomic beam.

Our initial results suggest that Alti and Khare's measurements were corrupted by contributions from multiply-scattered atoms that cross the laser beam at late times. Using their time-of-flight measurement methods, it was impossible to distinguish these atoms from those in the collimated beam. However, our experiment using velocity-sensitive laser spectroscopy measures the Doppler width and shift for atoms in the beam. We clearly see atoms at late times with an isotropic velocity distribution.

Chapter 2

Experimental Design and Setup

2.1 Setup

Our experiment is designed to run for long periods of time. Though Alti and Khare used Indium as their sample material we chose to use calcium, because we have the lasers necessary to characterize the atomic beam.

The entire two-stage ablation process is placed in a vacuum chamber (interior dimensions: 9.0" \times 12.75" \times 4.5"). This is necessary to create an atomic beam and prevents the Ca from oxidizing. We use a sapphire disk as our transparent substrate because sapphire has a high laser damage threshold and does not react rapidly with Ca. The thermal conductivity of Sapphire, $40 \text{ W m}^{-1} \text{ K}^{-1}$ at 20° C [2], is high enough that a small amount of energy of the back ablating YAG laser may be conducted away. However, the several second time constant for thermal conduction is much longer than the laser's ns pulse duration. In our setup there is no limit to the number of pulses of calcium that can be produced. Maintenance consists of smoothing the surface of the target approximately every 20 hours of run time using a lathe. Calcium is potentially combustible, and campus safety requires that we have a type-D fire extinguisher in

our laboratory.

2.1.1 Lasers

We use a frequency doubled Q-switched Nd:YAG laser at 532nm to ablate our calcium source. The laser has a peak unfocused fluence of $\sim 3 \text{ J/cm}^2$, pulse duration of 3 ns (FWHM), and a beam waist of about 0.5 cm. The YAG laser passes through an optical port into the chamber (appendix C).

Our 423 nm probe laser beam can be locked to the Ca resonance transition or scanned across a range of frequencies in order to obtain fluorescence from the atomic beam [3]. The probe laser beam polarization was changed from vertical to horizontal. We do this using an arrangement of 4 mirrors, as shown in Fig. 2.1.

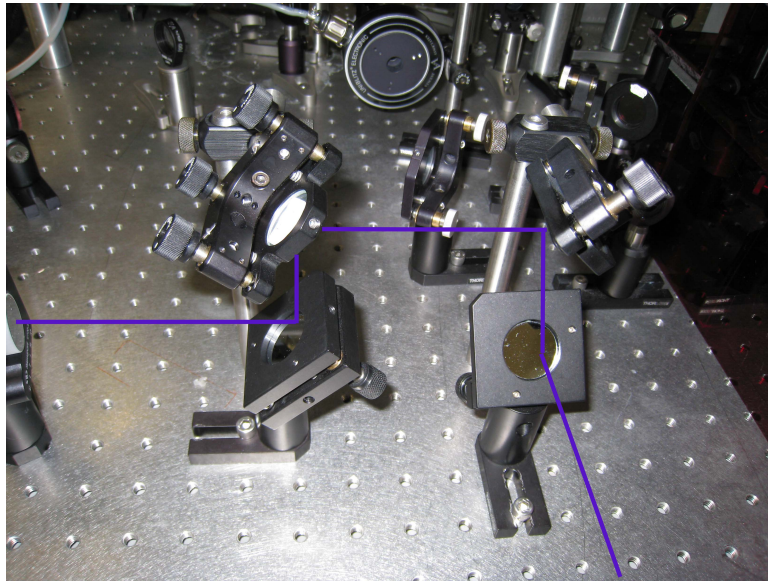


Figure 2.1 Four mirrors that take vertically polarized light and create horizontally polarized light. The blue lines indicate the path of the probe laser.

2.1.2 Internal Design

We use stepper motors to rotate and advance the calcium target and to rotate the sapphire disk. By counting the number of steps each motor takes, we can track the position of the calcium target. We use a mirror and lens to focus a YAG laser beam onto the Ca target. Another mirror is used to direct a weaker YAG laser beam onto the sapphire disk. In the initial design, the probe laser beam crosses the atomic beam at a right angle and is afterwards intercepted by a beam dump. If the probe laser beam is locked to the center of absorption line, then this configuration essentially eliminates the first-order Doppler shift. A thin film of Ca forms on the sapphire disk. The weaker YAG beam illuminates the sapphire disk from the back side, creating an atomic beam. Our design is shown in Fig. 2.2 below.

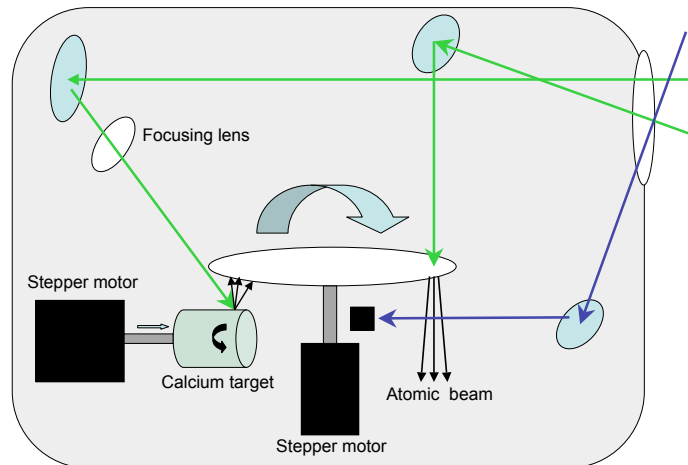


Figure 2.2 First setup for the vacuum chamber

We use custom mounts to hold the motors in place. (See diagrams in appendix C.) The mount for the Target motor is designed to move the Ca target forward and backward as the motor turns CW or CCW. This is done so that the YAG laser hits a

new spot with each pulse, preventing the laser from drilling a hole in the target and producing a more uniform ablation plume.

2.1.3 External Design

We used a Hamamatsu 1P28 photomultiplier tube (Appendix E) to measure the fluorescence of the atomic beam. The PMT was housed in an aluminum case with a tapped hole in one side to which we attached an anodized Al Thorlabs lens tube of length 140mm. At the end of the tube we placed a filter and a lens with a focal length of 75mm. The filter has a 20 nm bandpass centered at 420 nm. It is used to reject any scattered laser light. The lens was used for imaging the intersection of the atomic and probe laser beam onto the PMT photocathode. This allowed us to obtain a high signal to noise ratio. As mentioned previously, the YAG laser is split into two beams, one for ablating material off of the target and the other for back ablating the thin film on the disk. A beam splitting mirror was used to deflect 67% of the beam towards the target and transmit 33% to the thin film.

2.2 Vacuum Lid

The original lid for the vacuum chamber was made of plastic. The obvious advantage of a clear lid was that the entire chamber could be seen. Detectors could easily be repositioned wherever desired. Unfortunately the plastic lid did not allow a good enough vacuum in the chamber. The minimum pressure in the chamber was ~ 1 mTorr, far greater than the desired ~ 1 μ Torr.

We machined an aluminum lid with a viewport. The dimensions are: length - 14.500", width - 10.500", thickness - 0.750". Next we machined a smooth o-ring surface that held the lid in the proper position. The viewport is 1.500" in diameter

located 5.75" by 4.0" inward from the edges as shown in Fig. 2.3.

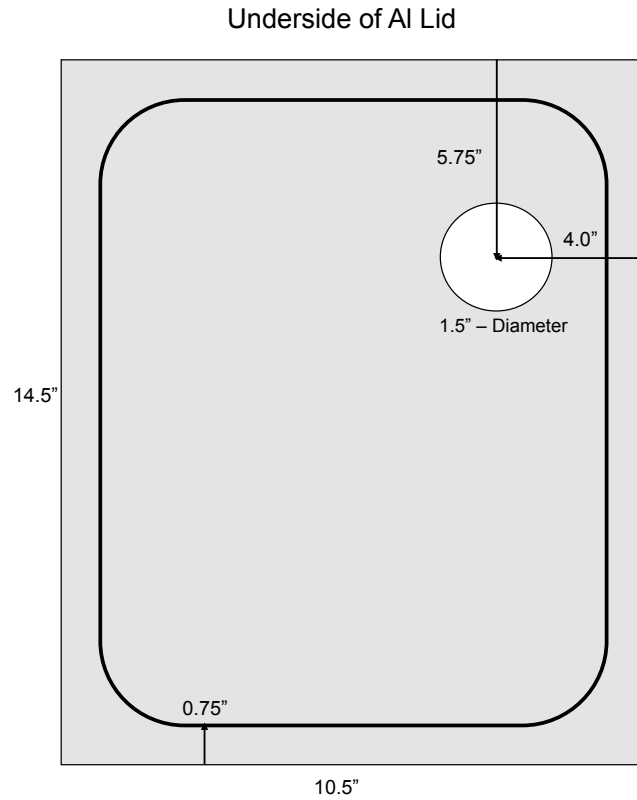


Figure 2.3 Dimensions for the Al lid

The vacuum chamber has a ring of tapped holes around the upper lip for bolts to hold a lid in place. Our original plan was to drill holes in the new Al lid for the bolts, but we saved time by simply letting the weight of the lid and atmosphere hold the lid down. We obtained a vacuum of $\sim 10 \mu\text{Torr}$. This made changes in the chamber quick and easy, because we only had to vent the system to be able to remove the lid. Unfortunately, the lack of mounting bolts made it impossible to backfill the chamber with gas. A future improvement to the lid could be made by drilling holes

for mounting bolts in the corners of the lid.

2.3 Control box and Labview program

The stepper motor drivers are model R208 microstepping drivers from Lin Engineering. See appendix B for informational schematics on stepper motors. The stepper motor models are 4118S-04S for the Ca target motor and 4118L-04S for Sapphire disk motor. We built the controls for the R208 drivers into a 19" rack mounted electronics enclosure (the control box). We cut holes for control switches and for coaxial cables to carry signals in and out.

We use the square-wave output from a Hewlett Packard 214B Pulse Generator (see Fig. 2.4) to drive the stepper motor controllers. This signal generator provides enough current and voltage for the R208 drivers. The output frequency of the generator in conjunction with the Stepper Resolution switches on the control box regulate the motors' speed.



Figure 2.4 The control box is sitting below the HP Signal Generator

The disk motor turns continuously while the experiment is running. We wrote a Labview program to control the movement of the Ca target. The program's front

panel was designed to be helpful and intuitive to users unfamiliar with our setup by showing exactly what the program is doing. See appendix A for a diagram of the program. The program counts the number of pulses sent to the motors. The number of pulses is proportional to how far the motors have turned in either direction. Once the target has moved the desired number of pulses in one direction the program sends the controller a different voltage (0 or 5.4 V) which reverses the motor direction. Without this program the target motor would get jammed at the end of its run and burn out. The program returns the target back to the starting position when a run of data is finished. It is important to let the motor finish this last step before turning off the power or turning off the program. The back of the controller has two manual override switches (Fig. 2.5). They allow a user to move the target motor manually.



Figure 2.5 Rear view of the control box

Chapter 3

Data

3.1 First Setup

A schematic diagram of our first experiment is shown in Fig. 2.2. This initial work focused on time-of-flight measurements and measured how long it took for the atomic beam pulse to cross the probe laser beam. The 423 nm fluorescence signal was detected using a PMT and recorded using a digital oscilloscope. We used neutral density filters to incrementally lower the power of our back-ablating YAG beam. This was done to test the claim of Alti and Khare [1] that their low temperature beam was created by using low intensity lasers. No significant amount of fluorescence could be detected when lowering our laser intensity beyond a factor of four. Our measurements showed no correlation between the velocity of the atoms and the intensity of the ablating laser beam. At lower intensity, the atomic beam became less intense but the time of flight remained essentially unchanged (see Fig. 3.3).

This setup was useful for testing the atoms' velocity in relation to the back ablating laser's power but it did not reveal the velocity components of the atomic beam.

3.2 Second Setup

Our present setup is designed to determine both the mean velocity and the velocity distribution of atoms in the pulsed atomic beam. We changed the alignment of the probe laser beam so that it crossed the atomic beam at an angle of 53° . A small mirror in the chamber retro-reflecting it straight back, as shown in Fig. 3.1.

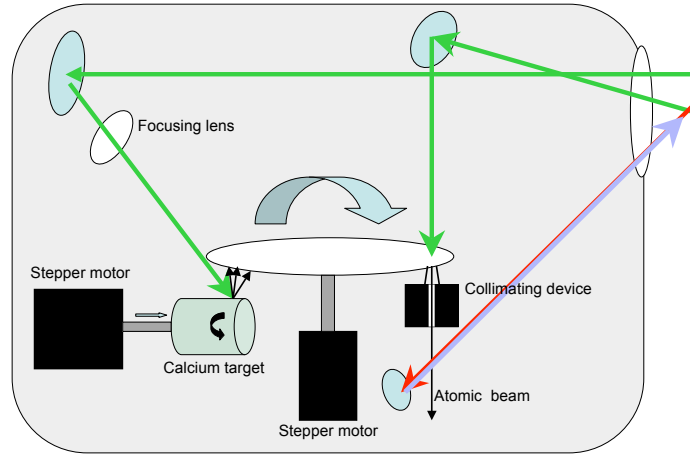


Figure 3.1 Second setup for the vacuum chamber

If the atomic and probe beams cross paths perpendicular to each other, the frequency required to excite electrons in the Ca to their first excitation level would be $\Delta f = 7.0922 \times 10^{11}$ GHz. But because the 423nm probe laser crossed the atomic beam at an angle the frequency that the atoms fluoresce was shifted by,

$$\Delta f = v \cos(\theta) / \lambda = 2.134 \times 10^9 \text{ Hz} \quad (3.1)$$

where $\lambda = 423 \times 10^{-9}$ m, $\theta = 53^\circ$, and axial velocity was arbitrarily chosen to be $v = 1500$ m/s. As we scan the probe laser frequency across the absorption line, we

see a blue-shifted and red-shifted peak, corresponding to absorption by the atoms of the incident and retro-reflected probe laser beam. The widths of these shifted peaks gives us the rms thermal velocity in the moving frame of the atomic beam. The shift between these peaks gives us the mean velocity of the beam. In some pulsed atomic sources, these two velocities are not the same.

3.3 Thermodynamics

Thermodynamic equations help us understand what is occurring in our Ca ablation source. Alti and Khare's In atomic beam had a claimed axial velocity of, $v = 44$ m/s, which corresponds to 8.9 K (appendix D). This counter-intuitive result seems to defy the laws of physics.

Relying on equations that Kadar-Kallen and Bonin present [4], we calculated that $E > 350$ mJ for significant ablation to occur. The maximum energy reported by Alti and Khare was 43.5 mJ.

In order to ablate material from any object, energy must be deposited more quickly than it dissipates. This requirement is expressed in equation (3.2). [4]

$$\chi \leq \frac{F}{\sqrt{t}}, \quad (3.2)$$

where χ is a figure of merit,

$$\chi = L \sqrt{\frac{K}{\rho C_p(s)}} \dots (\text{Jcm}^{-2}\text{s}^{-1/2}), \quad (3.3)$$

and L is energy/volume

$$L = \frac{\rho}{A} [\Delta_f H^\circ + (T - T_0) C_p(g)] \dots (\text{J}\mu\text{m}^{-1}\text{cm}^{-2}). \quad (3.4)$$

The following is a key for thermodynamic symbols.

F ... Laser fluence (J cm^{-2})

K ... Thermal conductivity ($\text{W m}^{-1} \text{K}^{-1}$)

T ... Gas temperature (K)

t ... Laser pulse width (s)

$C_p(g)$... Specific heat of gas ($\text{J mole}^{-1} \text{K}^{-1}$)

$C_p(s)$... Specific heat of solid ($\text{J kg}^{-1} \text{K}^{-1}$)

A ... Atomic weight (kg mole^{-1})

T_0 ... Solid Temperature (K)

$\Delta_f H^\circ$... Enthalpy of formation (kJ mole^{-1})

Our collimated unfocused YAG laser has a fluence $F = 3 \text{ J/cm}^2$, a pulse width of $t = 7 \text{ ns}$ FWHM, and a beam waist of about 0.5 cm . For Ca $\chi = 5.696 \times 10^4$, $L^{-1} = 1.242$, and $T = 1757$. $F/\sqrt{t} = 3.5856 \times 10^4$ is less than χ , so unless we focused the YAG we would not have seen ablation from the target. Ablation from the target would begin when the laser is focused to at least 0.2 cm , but the ablation plume would not be very dense. We placed a 90 mm lens in our chamber to focus the YAG laser onto the target. Supposing our YAG laser was perfectly Gaussian, which it isn't, we would have obtained a beam waist, according to equation (3.5), of $3 \mu\text{m}$. The actual beam waist may be significantly larger, but we did not measure it. It seems likely that it is in the range of $100 \mu\text{m}$. The beam waist at the focus, W_f can be calculated if the initial beam waist at the lens, W_0 , is known,

$$W_f = \frac{\lambda f}{\pi W_0}. \quad (3.5)$$

Our initial beam waist is $W_0 = 5.0 \text{ mm}$ before it passes through the lens, $\lambda = 532 \text{ nm}$, and $f = 90 \text{ mm}$. The beam that ablates material off of the target is 67% of the original 3 J/cm^2 YAG beam. If it has a beam waist of $100 \mu\text{m}$ then the fluence is $F = 5025 \text{ J/cm}^2$.

3.4 Data

Data from the first setup indicate that sub-thermal atomic beams using two stage laser ablation are not possible. Three plots of data from this setup are shown below. All data reduction of our measurements was carried out in Matlab.

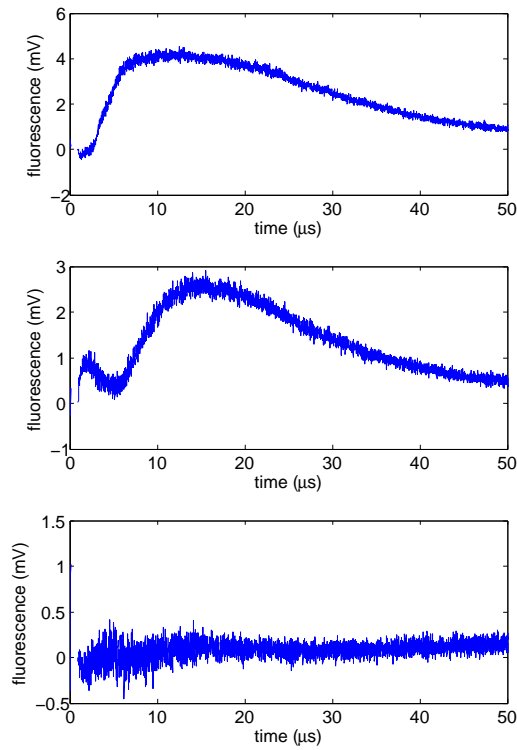


Figure 3.2 Graph of fluorescence vs. time for atoms in the first setup. The point of measure for this graph is 3.5 cm from the sapphire disk. The back-ablating intensity is $I = 0.99 \text{ J/cm}^2$ (top panel), $I = 0.248 \text{ J/cm}^2$ (middle panel), and $I = 0.198 \text{ J/cm}^2$ (bottom panel). For the weakest intensity, only noise is visible.

Measurements from the second setup show us something very similar to what Alti and Khare observed in their experiment [1] (see ??). We measured two peaks

in fluorescence in the beam, one for atoms traveling around 1500 m/s and another one for atoms traveling around 100 m/s (see Fig. 2.2). The 100 m/s signal is caused by multiply scattered or ablated atoms and a low density Ca gas that formed from ablation on the Ca target and the sapphire disk. The multiply scattered atoms are most easily observed when the collimating device is in place. Atoms deposited on the surface of the device from back ablations of the sapphire disk get illuminated with the YAG laser when it shines through the disk and ablate off.

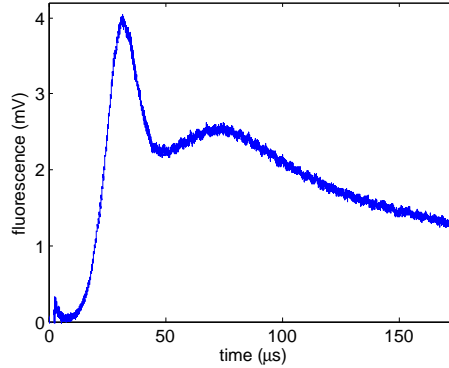


Figure 3.3 Graph of fluorescence vs. time for atoms in the second setup. The point of measure for this graph is 4.0 cm from the sapphire disk. The prompt peak from atoms in the collimated beam is clearly seen on top of a broad background from isotropically scattered atoms.

Chapter 4

Conclusion

4.1 Conclusions

Our initial measurements suggest that Alti and Khare's measurements were corrupted by contributions from multiply-scattered atoms that cross the laser beam at late times. Using only their time-of-flight measurement methods, there is no way to distinguish these atoms from those in the collimated beam. However, using velocity-sensitive laser spectroscopy and measuring the Doppler width and shift, we clearly see these "slow" atoms. Initial measurements have shown that there is no correlation between the axial velocity of an atomic beam and the intensity of the back ablating laser. Further research and more measurements must be performed in the second setup to conclusively show that Alti and Khare's methods and results were incorrect.

Bibliography

- [1] K. Alti and A. Khare, Review of Scientific Instruments **76**, 113302 (2005).
- [2] C. SA, <http://www.azom.com/news.asp?ArticleID=3382> (Accessed April 14, 2008).
- [3] E. A. Cummings, J. E. Daily, D. S. Durfee, and S. D. Bergeson, Physical Review Letters **95**, 235001 (2005).
- [4] M. A. Kadar-Kallen and K. D. Bonin, Applied Physics Letters **64**, 1436 (1994).

Appendix A

Labview program for running the
target stepper motor

Stepper driver.vi
P:\Research\CA Ablation Project\Stepper driver.vi
Last modified on 3/14/2008 at 6:46 PM
Printed on 4/15/2008 at 4:28 PM

Page 1

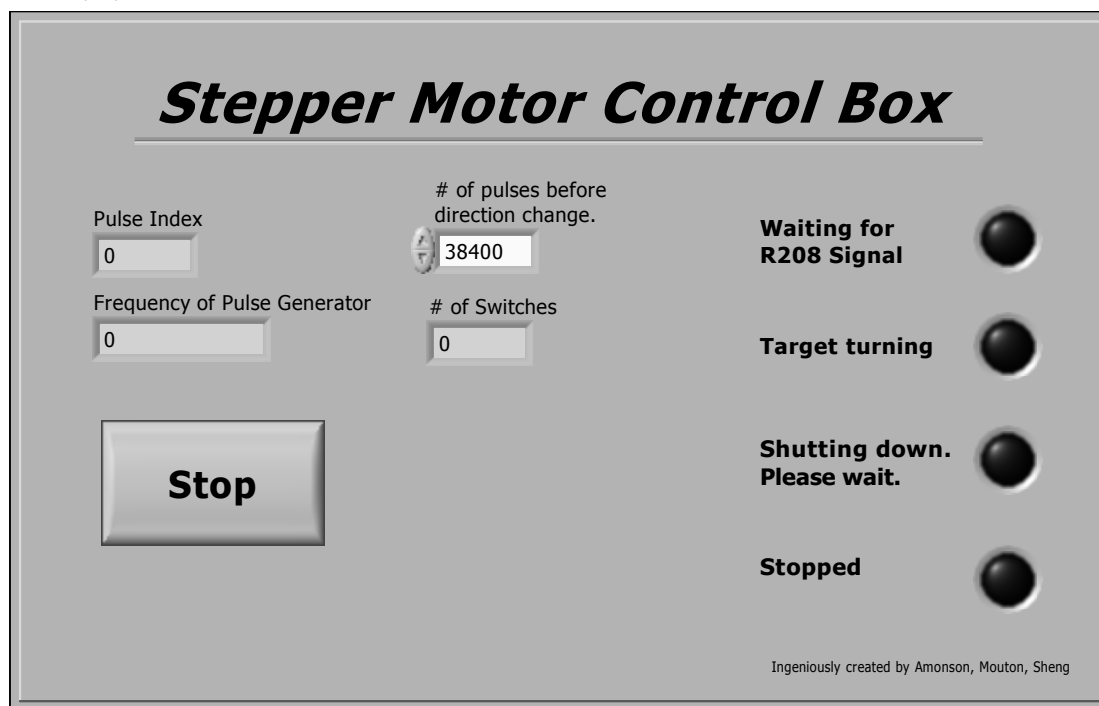


Figure A.1 Front panel for the control program

Stepper driver.vi
P:\Research\CA Ablation Project\Stepper driver.vi
Last modified on 3/14/2008 at 6:46 PM
Printed on 4/15/2008 at 4:47 PM

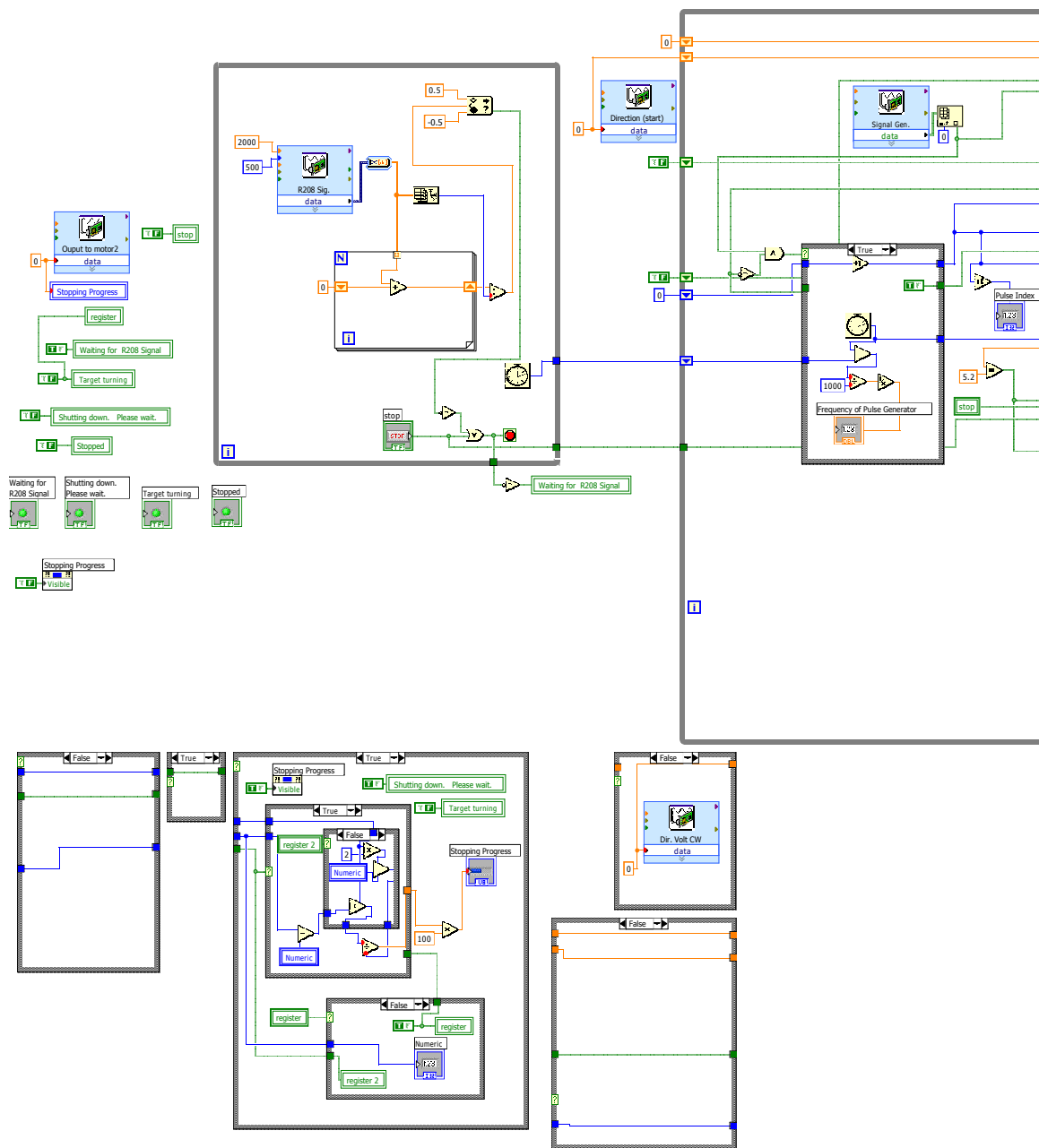


Figure A.2 Diagram of program

Stepper driver.vi
P:\Research\CA Ablation Project\Stepper driver.vi
Last modified on 3/14/2008 at 6:46 PM
Printed on 4/15/2008 at 4:48 PM

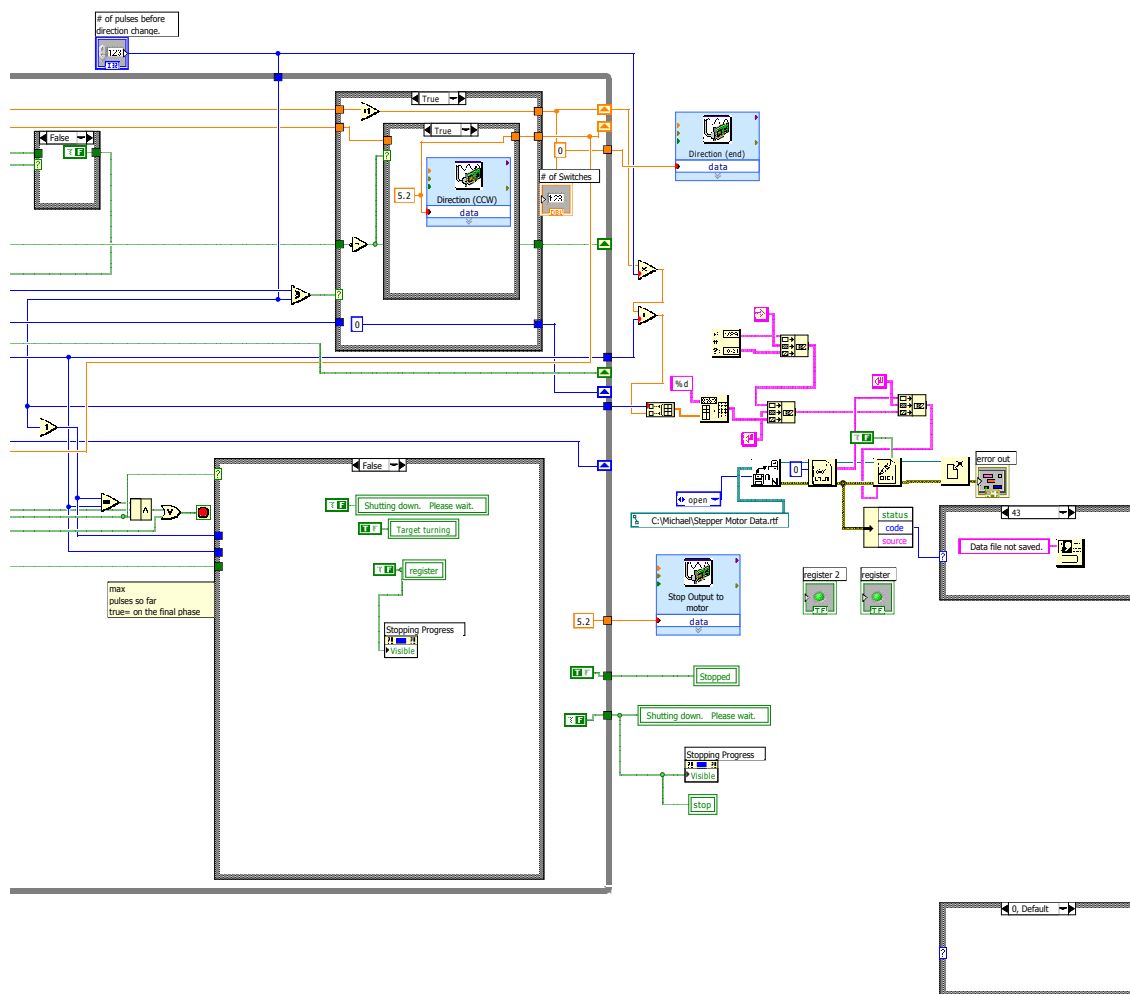


Figure A.3 Diagram of program

Stepper driver.vi
P:\Research\CA Ablation Project\Stepper driver.vi
Last modified on 3/14/2008 at 6:46 PM
Printed on 4/15/2008 at 4:48 PM

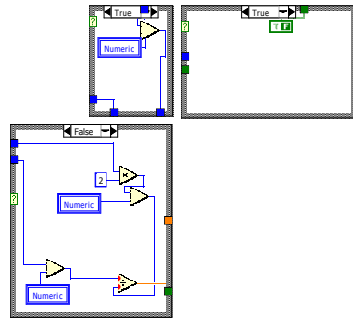


Figure A.4 Diagram of program

Appendix B

Schematics for the stepper motors

Model #	Frame Size	Length (in)	Volts	Current (Amps)	Holding Torque (oz-in)	Resistance (ohms)	Inductance (mH)
4118L-04S	17	1.89	6.79	0.87	82.80	7.80	13.84
					Rotor Inertia (oz-in ²)	Weight (lbs)	Lead wires
					0.37	0.70	4

Torque Curve:

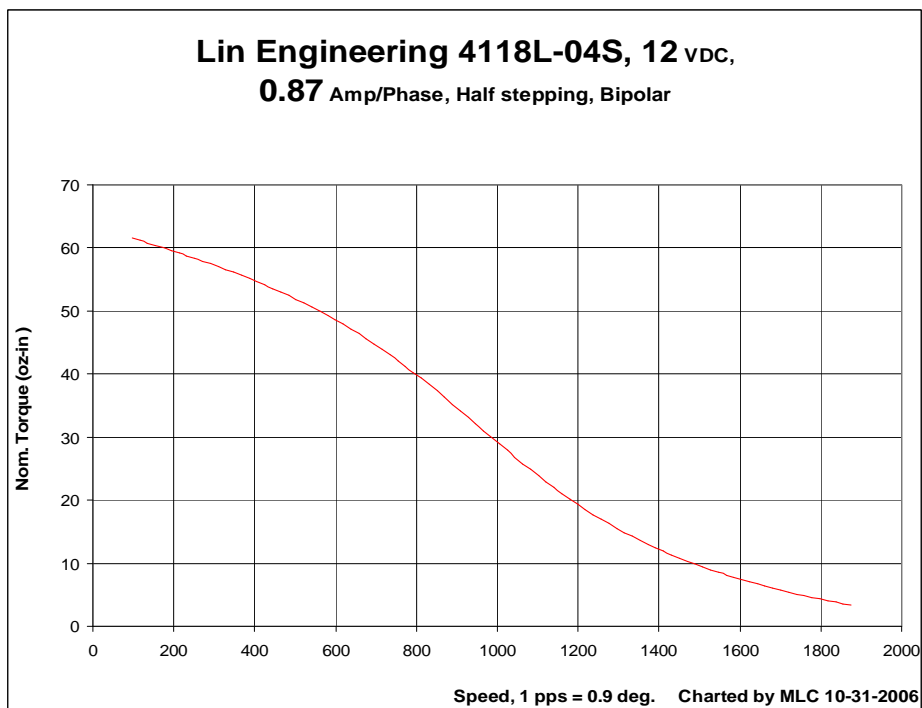


Figure B.1 Motor that turns the sapphire disk

Model #	Frame Size	Length (in)	Volts	Current (Amps)	Holding Torque (oz-in)	Resistance (ohms)	Inductance (mH)
4118S-04S	17	1.34	6.66	0.67	34.22	9.94	12.52
					Rotor Inertia (oz-in ²)	Weight (lbs)	Lead wires
					0.18	0.40	4

Torque Curve:

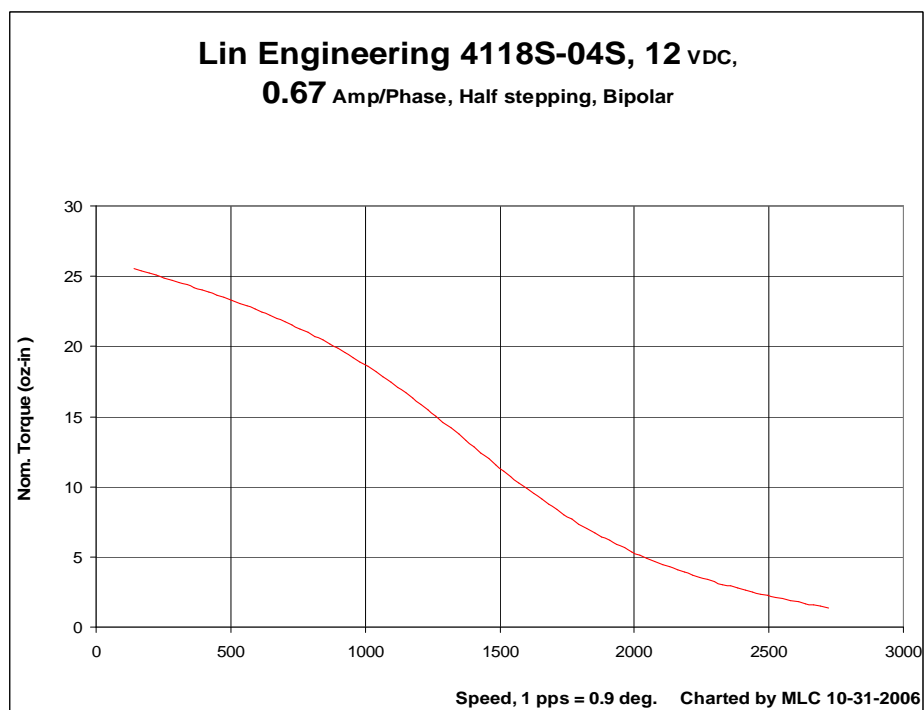


Figure B.2 Motor that turns the target

Appendix C

Motor mounts

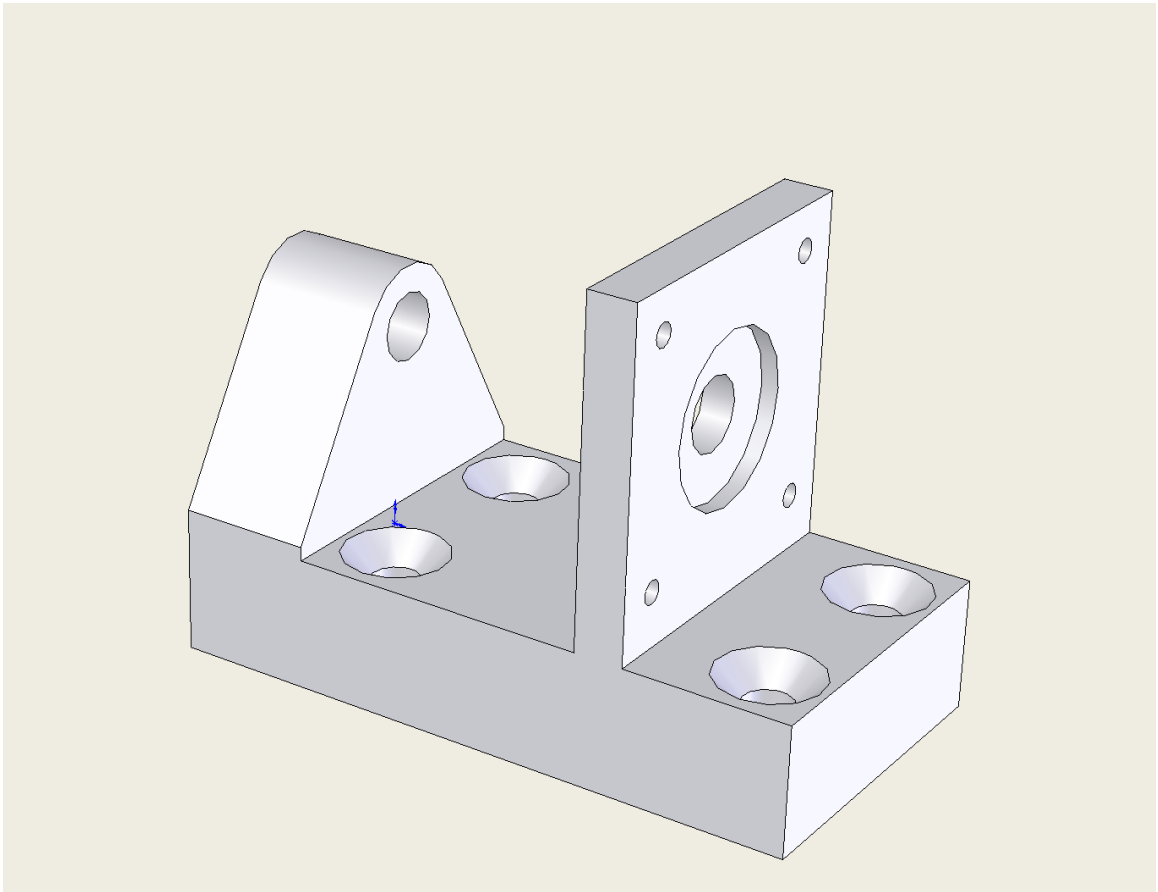


Figure C.1 Mount for the target motor

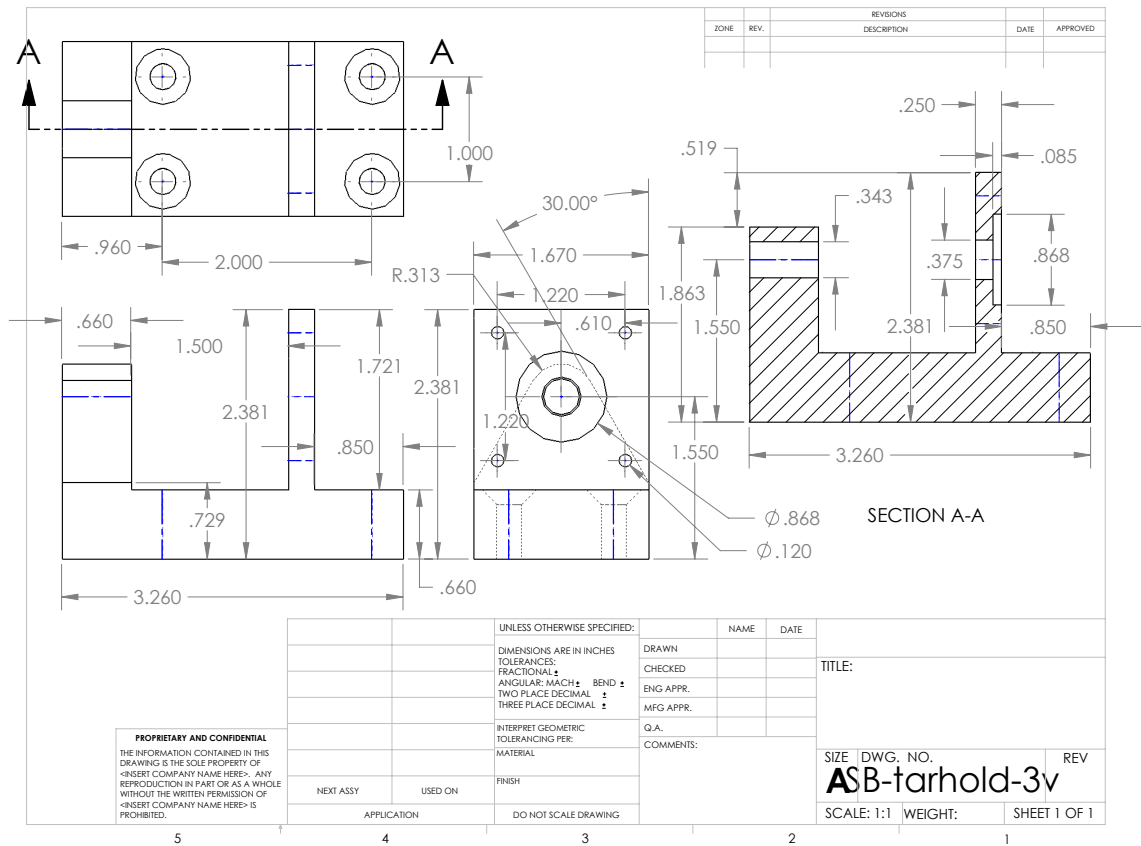


Figure C.2 Dimensions for target motor mount

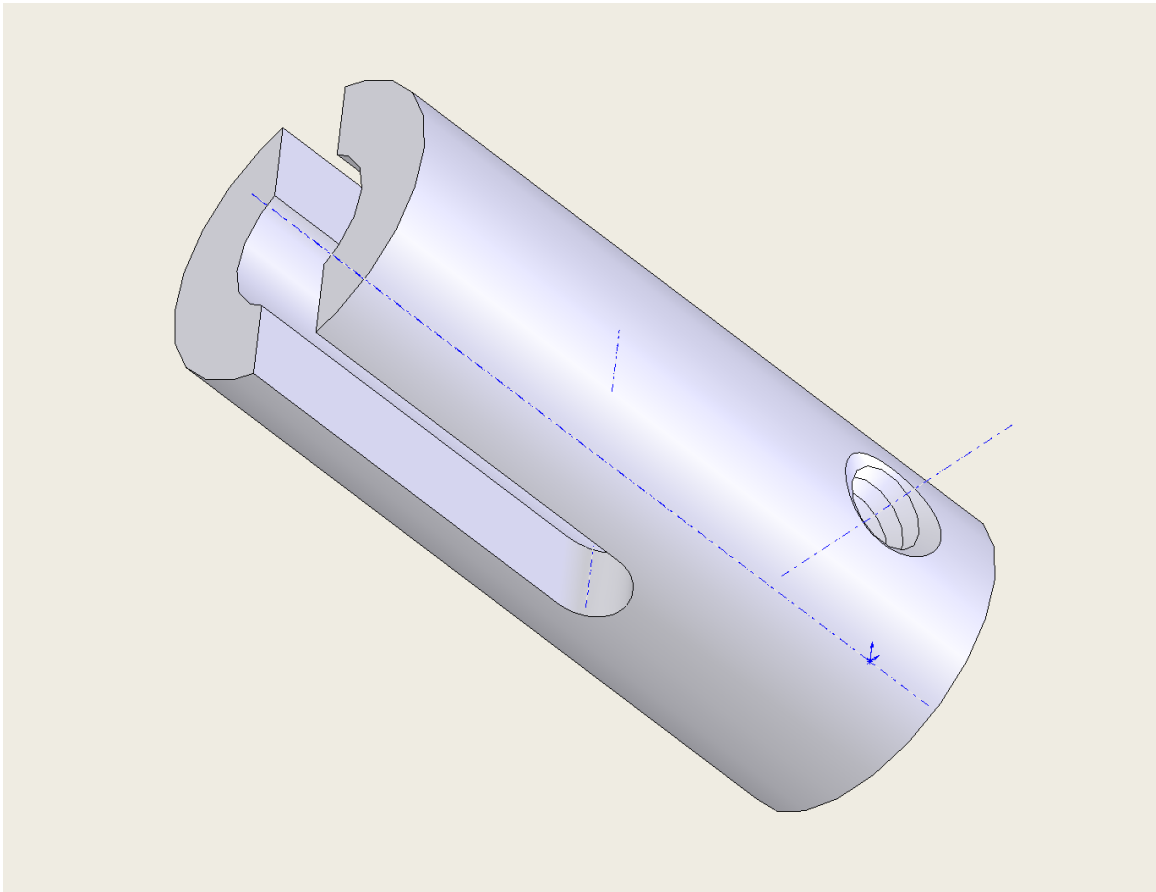


Figure C.3 The Holder is tightened onto the motor target motor's shaft.
The

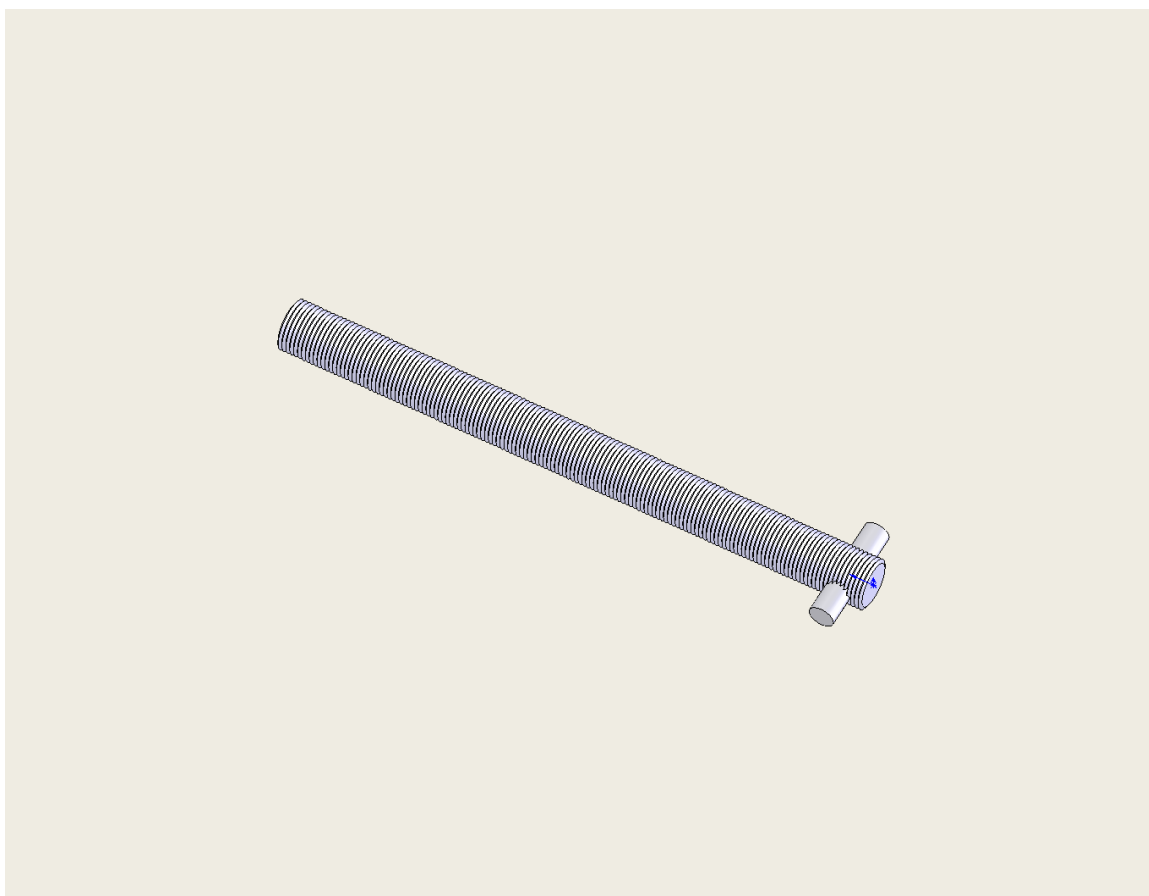


Figure C.4 Rod that the Ca target is placed on. It sits inside the holder. The threads on the rod advance the target with each step of the motor.

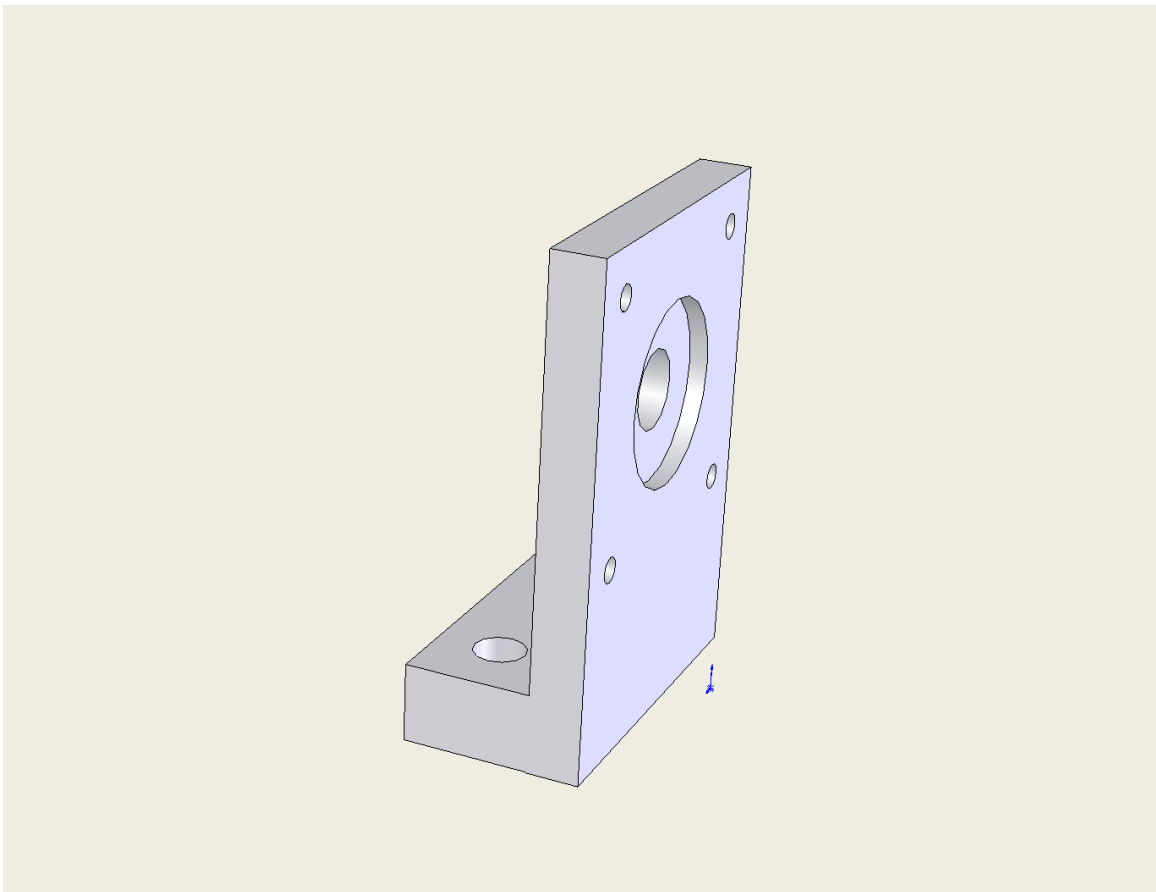


Figure C.5 Mount for the disk motor

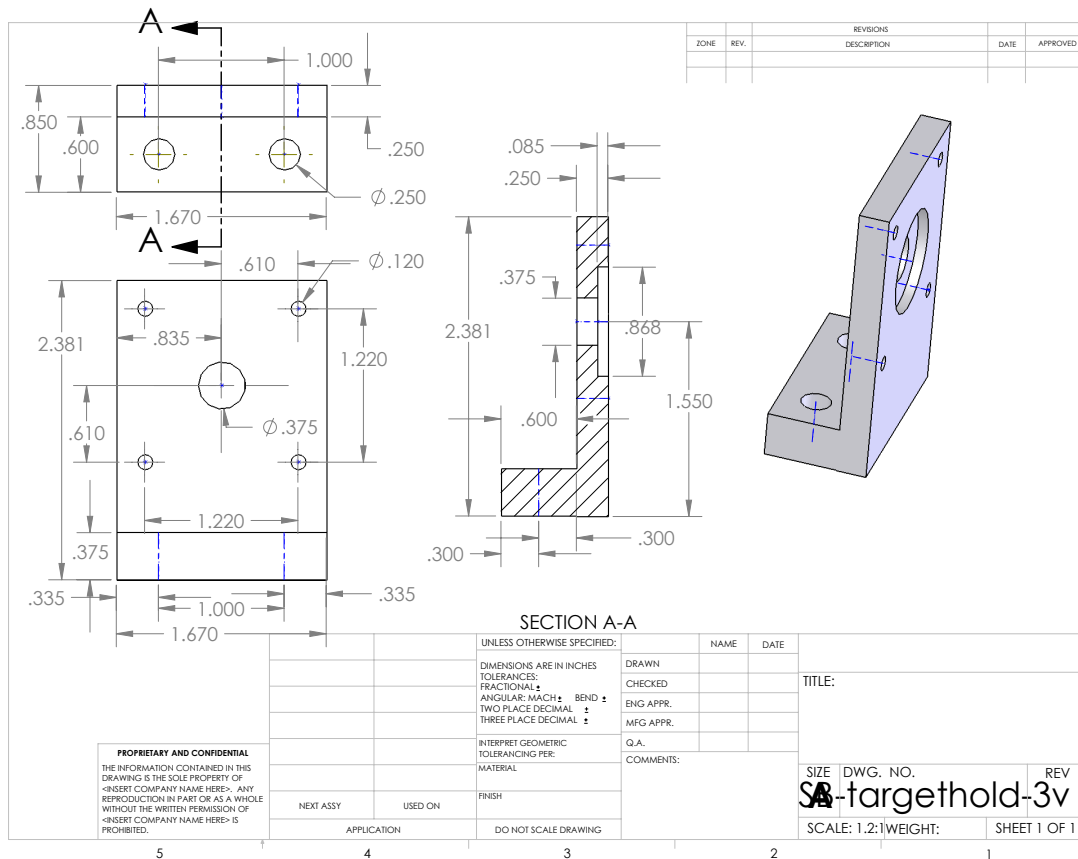


Figure C.6 Dimensions for disk motor mount

Appendix D

Maple work and formulae

```

Indium
> restart;
> k:=81.8; rho:=7310; T:=2345; T0:=298; Cg:=20.8; Cs:=26.7; A:=
  .114818; H:=243300;
      k := 81.8
      ρ := 7310
      T := 2345
      T0 := 298
      Cg := 20.8
      Cs := 26.7
      A := 0.114818
      H := 243300
(1)
> L:=rho/A*(H+(T-T0)*Cg);
      L := 1.820067634 1010
(2)
Units of Joules/m^3
> 1/L;
      5.494301318 10-11
(3)
> modL:=1/L*10^6*100^2;
      modL := 0.5494301318
(4)
Units of micrometers*cm^2/Joules
> chi:=L*sqrt(k/(rho*Cs));
      χ := 3.726060133 108
(5)
Units of Joules/(m^2*s^(1/2))
> modchi:=chi/10000;
      modchi := 37260.60133
(6)
Units of Joules/(cm^2*s^(1/2))
>
>
> laserpower:=.3/(5*10^(-9));
      laserpower := 6.00000000 107
(7)
Units of Wats
> 3/.6;
      5.000000000
(8)
> evalf(1.75/sqrt(8*10^(-9)));
      19565.59480
(9)
This is the fluence per second of the unfocused beam divided by the sqrt of 7 nanoseconds.
Units of J/(cm^2*s^(1/2)). This is not enough to achieve ablation according to F/sqrt(t)>= chi.
>

```

Figure D.1

```
Alti & Khare's claimed indium velocity & temperature
> restart;
> kb:=1.38065e-23; T:=300; mass_In:=114.82*1.660538782e-27;
      kb := 1.38065 10-23
      T := 300
      mass_In := 1.906630629 10-25
(1)
> v:=sqrt(3/mass_In*kb*T);
      v := 255.2876295
(2)
This is the approximate velocity in m/s of In atoms in a gaseous state.

The following lines of code use Alti and Khare's lowest and highest
claimed atomic velocity to determine the atoms' temperature.
> v2:=44;
      v2 := 44
(3)
> T2:=v2^2*mass_In/(3*kb);
      T2 := 8.911833553
(4)
> v3:=100;
      v3 := 100
(5)
> T3:=v3^2*mass_In/(3*kb);
      T3 := 46.03219810
(6)
Temperature in Kelvin.
>
```

Figure D.2

```

Calcium
> restart;
> k:=201: rho:=1550: T:=1757: T0:=298: Cg:=20.8: Cs:=25.9: A:=
  .040078: H:=177800:
> L:=rho/A*(H+(T-T0)*Cg);
                                     L := 8.050006487 109          (1)
Units of Joules/m^3
> 1/L;
                                     1.242235024 10-10          (2)
> modL:=1/L*10^6*100^2;
                                     modL := 1.242235024          (3)
Units of micrometers*cm^2/Joules
> chi:=L*sqrt(k/(rho*Cs));
                                     χ := 5.696112105 108          (4)
Units of Joules/(m^2*s^(1/2))
> modifiedchi:=chi/10000;
                                     modifiedchi := 56961.12105          (5)
Units of Joules/(cm^2*s^(1/2))
> laserpower:=.3/(7*10^(-9));
                                     laserpower := 4.285714286 107          (6)
Units of Watts or J/s.
> Fluence:=3: t:=7e-9:
> evalf(Fluence/sqrt(t));
                                     35856.85828          (7)
This is the fluence per second of the unfocused beam divided by the sqrt of 7 nanoseconds.
Units of J/(cm^2*s^(1/2)). This is not enough to achieve ablation according to
F/sqrt(t) >= modifiedchi.
> d:=evalf(16500/L);
                                     d := 0.000002049687790          (8)
This is the approximate thickness of substrate that can be back ablated. units in meters.
> evalf(3*Pi*.5^2);
                                     2.356194490          (9)
>

```

Figure D.3

Detected calcium velocity and temperature

```
> restart;
> kb:=1.38065e-23; mass_Ca:=40.078*1.660538782e-27;
      kb := 1.38065 10-23
      mass_Ca := 6.655107330 10-26 (1)
> v1:=1300;
      v1 := 1300 (2)
> T1:=v1^2*mass_Ca/(3*kb);
      T1 := 2715.419401 (3)
> v2:=1500;
      v2 := 1500 (4)
> T2:=v2^2*mass_Ca/(3*kb);
      T2 := 3615.203343 (5)
> v3:=1700;
      v3 := 1700 (6)
> T3:=v3^2*mass_Ca/(3*kb);
      T3 := 4643.527850 (7)
All velocities are shown in meters/second and temperature in Kelvin.
>
```

Figure D.4

Doppler Shifting

```
> restart;
> f:=3e14/423;
                                     f:= 7.092198582 1011 (1)
This is the frequency of the first transition of Ca atoms in the atomic beam if we impinged the
blue laser perpendicular to the beams forward velocity vector.
> df_straight:=1500/423e-9;
                                     df_straight := 3.546099291 109 (2)
This would be the change in frequency if the blue laser was aimed parallel down the path of the
atomic beam.
> v:=1500: theta:=53*Pi/180:
> v_sr:=evalf(v*cos(theta));
                                     v_sr:= 902.7225348 (3)
> lambda:=423e-9:
> df:=v_sr/lambda;
                                     df:= 2.134095827 109 (4)
This is the approximate change in frequency for the atomic beam.
>
```

Figure D.5

Appendix E

Hamamatsu 1P28 Photomultiplier Tube

HAMAMATSU

PHOTOMULTIPLIER TUBE 1P28

FEATURES

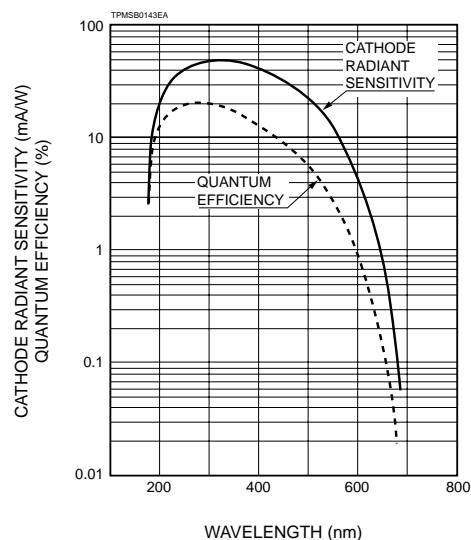
- 28mm (1-1/8 Inch) Diameter Side-on
- 185 to 650nm Spectral Response
- For UV to Visible Range Photocathode



GENERAL

Parameter		Description/Value	Unit
Spectral Response		185 to 650	nm
Wavelength of Maximum Response		340	nm
Photo-cathode	Material	Sb-Cs	—
	Minimum Useful Size	8 × 24	mm
Window Material		UV glass	—
Dynode	Structure	Circular-cage	—
	Number of Stages	9	—
Direct Interelectrode Capacitances	Anode to Last Dynode	4	pF
	Anode to All Other Electrodes	6	pF
Base		JEDEC No. B11-88	—
Suitable Socket		E678-11A	—

Figure 1: Typical Spectral Response



Subject to local technical requirements and regulations, availability of products included in this promotional material may vary. Please consult with our sales office. Information furnished by HAMAMATSU is believed to be reliable. However, no responsibility is assumed for possible inaccuracies or omissions. Specifications are subject to change without notice. No patent rights are granted to any of the circuits described herein. © 1999 Hamamatsu Photonics K.K.

Figure E.1

PHOTOMULTIPLIER TUBE 1P28

MAXIMUM RATINGS (Absolute Maximum Values)

Parameter	Value	Unit	
Supply Voltage	Between Anode and Cathode	1250	Vdc
	Between Anode and Last Dynode	250	Vdc
Average Anode Current	0.1	mA	
Ambient Temperature	-80 to +50	°C	

CHARACTERISTICS (at 25°C)

Parameter	Min.	Typ.	Max.	Unit
Anode Sensitivity	Luminous (2856K)	20	400	A/lm
	Radiant at 400nm	—	4.8×10^5	A/W
Cathode Sensitivity	Luminous (2856K)	25	40	$\mu\text{A/lm}$
	Radiant at 400nm	—	48	mA/W
Quantum Efficiency at 340nm	—	21	—	%
Gain	—	1.0×10^7	—	—
Anode Dark Current (after 30 minute)	—	5	50	nA
Time Response	Anode Pulse Rise Time	—	2.2	ns
	Electron Transit Time	—	22	ns

VOLTAGE DISTRIBUTION RATIO AND SUPPLY VOLTAGE

Electrodes	K	Dy1	Dy2	Dy3	Dy4	Dy5	Dy6	Dy7	Dy8	Dy9	P
Ratio	1	1	1	1	1	1	1	1	1	1	1

Supply Voltage: 1000Vdc, K: Cathode, Dy: Dynode, P: Anode

Figure 2: Typical Gain Characteristics

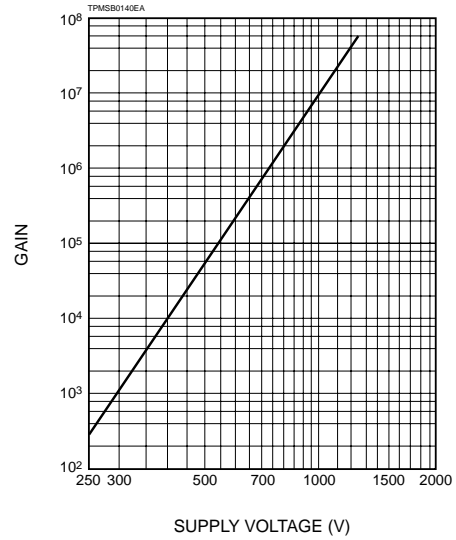
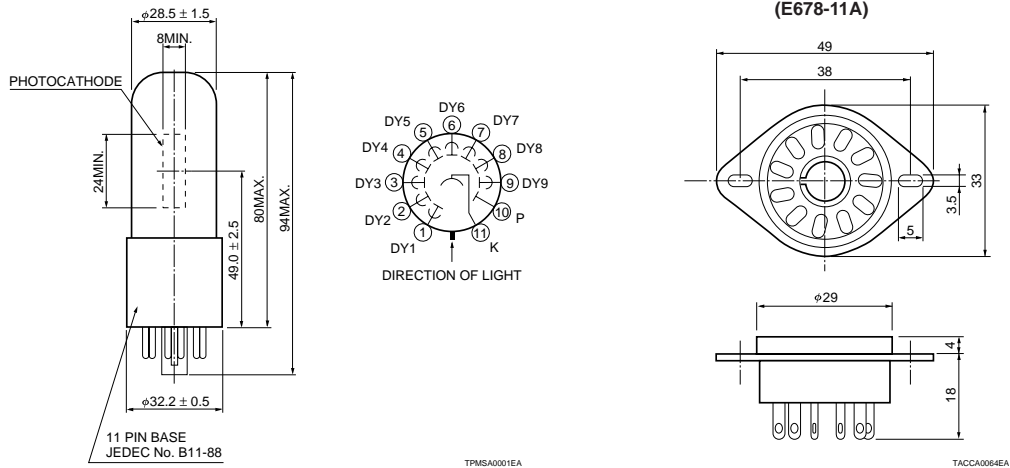


Figure 3: Dimensional Outline and Basing Diagram (Unit: mm)



HAMAMATSU

HAMAMATSU PHOTONICS K.K., Electron Tube Center

314-5, Shimokanzo, Toyooka-village, Iwata-gun, Shizuoka-ken, 438-0193, Japan, Telephone: (81)539/62-5248, Fax: (81)539/62-2205

U.S.A.: Hamamatsu Corporation: 360 Foothill Road, P. O. Box 6910, Bridgewater, N.J. 08807-0910, U.S.A., Telephone: (1)908-231-0960, Fax: (1)908-231-1218

Germany: Hamamatsu Photonics Deutschland GmbH: Arzbergerstr. 10, D-82211 Herrsching am Ammersee, Germany, Telephone: (49)8152-375-0, Fax: (49)8152-2658

France: Hamamatsu Photonics France S.A.R.L.: 6, Rue du Saule Trapu, Parc du Moulin de Massy, 91802 Massy Cedex, France, Telephone: (33)1 69 53 71 00, Fax: (33)1 69 53 71 10

United Kingdom: Hamamatsu Photonics UK Limited: Lough Point, 2 Glasbeck Way, Windmill Hill, Enfield, Middlesex EN2 7JA, United Kingdom, Telephone: (44)181-367-3560, Fax: (44)181-367-6384

North Europe: Hamamatsu Photonics Norden AB: Smidesvägen 12, SE-171-41 SOLNA, Sweden, Telephone: (46)8-509-031-00, Fax: (46)8-509-031-01

Italy: Hamamatsu Photonics Italia: S.R.L.: Strada della Moia, 1/E, 20020 Arese, (Milano), Italy, Telephone: (39)02-935 81 733, Fax: (39)02-935 81 741

TPMS1062E01
FEB. 1999

Figure E.2

Appendix F

Additional information about the vacuum chamber's window ports

The chamber has two window ports on opposite walls, one 1.5" in diameter and the other 0.69". We used the larger window for the YAG laser (532nm) and the smaller window for a probe beam (423nm). After purchasing two anti-reflection coated windows for the chamber, we were informed that the smaller window port had broken two previous windows during installation. We checked for unevenness in the window port and for gouges or nicks in the metal. We also sanded the area down to ensure a flat uniform surface. It was all to no avail though. After we tightened down the holding piece for the port the window broke. It remains a mystery to this day why it has broken so many windows. The windows we purchased each cost around \$500, so we decided against another attempt and put a piece of aluminum in place of the window. Luckily the anti-reflection coating on the 1.5" window had an acceptable reflectance range for both lasers $< 10\%$.

Index

Background, 1
Conclusions, 16
Data, 14
External Design, 6
First setup, 10
Internal Design, 5
Labview and control box, 8
Lasers, 4
Lid, 6
Second setup, 11
Setup, 3
Thermodynamics, 12